ANTIOXIDANTS & REDOX SIGNALING
Volume 9, Number 8, 2007

DOI: 10.1089/ars.2007.1634

Forum Review

Brain Tissue Oxygen Concentration Measurements

OBINNA NDUBUIZU and JOSEPH C. LAMANNA

ABSTRACT

Brain function depends exquisitely on oxygen for energy metabolism. Measurements of brain tissue oxygen tension, by a variety of quantitative and qualitative techniques, going back for >50 years, have led to a number of significant conclusions. These conclusions have important consequences for understanding brain physiology as it is now being explored by techniques such as blood-oxygen-level–dependent functional magnetic resonance imaging (BOLD *f*MRI) and near-infrared spectroscopy (NIRS). It has been known for some time that most of the measured oxygen tensions are less than venous pO_2 and are distributed in a spatially and temporally heterogeneous manner on a microregional scale. Although certain large-scale methods can provide reproducible average brain pO_2 measurements, no useful concept of a characteristic oxygen tension or meaningful average value for brain tissue oxygen can be known on a microregional level. Only an oxygen field exists with large local gradients due to local tissue respiration, and the most useful way to express this is with a pO_2 distribution curve or histogram. The neurons of the brain cortex normally exist in a low-oxygen environment and on activation are oxygenated by increases in local capillary blood flow that lead to increases in hemoglobin saturation and tissue oxygen. *Antioxid. Redox Signal.* 9, 1207–1219.

INTRODUCTION

OXYGEN IS AN ESSENTIAL NUTRIENT. Because of its reactive nature, oxygen is useful as an electron acceptor during energy metabolism, but it is also a potent toxin. This duality means that for all tissues, risks are involved if oxygen levels become too high or too low and, thus, a range of oxygen concentrations exists that is optimal to support effective function. Effective mechanisms regulate oxygen tension in tissues.

Advanced organisms extract oxygen from the surroundings for distribution to tissues and cells to serve as the final electron acceptor during mitochondrial oxidative phosphorylation and also as a participant in other biochemical reactions. These processes have been evolutionarily conserved through the development of advanced multilevel systems, which tightly maintain oxygen homeostasis within narrow physiologic ranges in various tissues and cells (1). The range of optimal oxygen concentrations in the mammalian brain has not been fully appreciated or determined, primarily because the tools and techniques for quantitative oxygen measurements in the awake, normally functioning brain have been limited, mostly by the need for noninvasiveness. In addition, both temporal and spatial heterogeneities at the microregional level require adequate response time and signal localization in whatever methods are used. Nevertheless, that an optimal range exists is undoubted. In the face of imposed increases or decreases of oxygen, specific consequences and adapting mechanisms are triggered. The mammalian brain is a highly aerobic organ with very small energy stores, making neuronal activity and energy metabolism greatly dependent on constant oxygen and glucose delivery. It should not be surprising, therefore, that neuronal activity, blood flow, glucose consumption, and capillary density are all tightly correlated. Extreme decreases in oxygen availability cannot be tolerated for long periods because the energy supplied from anaerobic glycolysis is insufficient to maintain viability (1).

Oxygen is required for the production of reactive oxygen species, which contribute to physiologic processes such as the regulation of cerebral blood flow. Reactive oxygen species also

[1]Departments of Physiology and Anatomy, Case Western Reserve University, Cleveland, Ohio.

play a role in mediating cellular damage after ischemia and other insults (18). Excessive amounts of oxygen increase the risk of cell injury through oxidative stress. Neurons are especially vulnerable to the deleterious effects of reactive oxygen species because they have limited capacity, if any, for cell division or regeneration.

Thus, elaborate oxygen-sensing mechanisms are present in mammals to regulate oxygen homeostasis tightly in the CNS to minimize the risk of metabolic compromise or excessive oxidative stress. With the brain receiving 15–20% of the total cardiac output and accounting for 20% of the total body metabolism (although only constituting ~2% of total body weight), it is well known that oxygen deprivation during severe hypoxia and ischemia leads to energy failure and neuronal death. Therefore, an important question to consider is the critical oxygen-tension level at which homeostasis for cellular energetics begins to fail.

Historically it has been difficult to evaluate brain oxygen tension *in vivo* and even more difficult to assess in conscious unanesthetized animals or humans or both. Strides have been made over the last half century to improve methods for assessing brain oxygen tension *in vivo*. We review the methods that have been used for quantitative estimates of brain tissue oxygen concentration and discuss the implications of spatial and temporal heterogeneity of microregional oxygen tension in the brain.

QUANTITATIVE METHODS

Measurements of oxygen have been made by methods that take advantage of the chemical and physical characteristics specific to oxygen (Table 1). These methods fall into the categories of polarography, optical, electron paramagnetic resonance (EPR), nuclear magnetic resonance (NMR), positron emission tomography (PET), and mass spectrometric. Indirect signals of oxygen concentration also are used, including hemoglobin saturation, cytochrome oxidase redox state, and NADH redox state. None of these singly at present provides all the data needed to delineate fully the *in vivo* distribution of oxygen in brain. The methods vary in terms of their ease of use, expense, invasiveness, sensitivity, and resolution (spatial and temporal).

Polarography

Most of the existing brain tissue pO_2 data were generated with polarographic microelectrodes. Polarography involves the reduction of oxygen at the surface of a noble metal under the influence of negative polarizing voltage. The methodologic background has been described in detail by Vanderkooi (97). The polarographic electrode usually consists of a membrane-covered cathode where oxygen is reduced and a nearby or integral reference electrode. In this system, the cathode transfers electrons to oxygen, producing a current proportional to the concentration of oxygen adjacent to the electrode and the reactive surface of the electrode.

In the early 1940s, Davies and Brink (4) showed that oxygen-measuring polarographic electrodes could be used in animals to obtain reliable and repeatable data. They used 25-μm-diameter, recessed-tip, glass-covered platinum electrodes. They also compared the data from these electrodes with those from small, open-tip electrodes, which were much faster responding but could not be quantitatively calibrated. It was not until the reports by Davies and Bronk (15) that quantitative measurements were first reported. Almost all of the oxygen tensions recorded by these investigators, from anesthetized cat cortex, were below the oxygen tensions they found in the surface veins. The tissue oxygen tensions characteristically varied from 2 to 10 torr, which variation they attributed to the differences in capillary proximity. They concluded that "many cortical locations have oxygen tension values nearly low enough to cause metabolic impairment." They also reported the observation that the measured oxygen tension decreased to a plateau that did not reach zero oxygen during anoxic exposure. This "nonzero" value could have been due to a limitation of the electrodes or a small residual amount of oxygen remaining present (reduced oxygen consumption).

In the 1950s, Clark (10) enhanced the performance and consistency of electrodes for use in biologic fluids and tissues by electrically insulating the anode and cathode with a gas-permeable, but not liquid-permeable, membrane. This provided a more stable environment for the electrode reaction and more closely defined the diffusion conditions to that surface. The application of the membrane prevented the reduction of other molecules in the medium and reduced the sensitivity to fluid motion in the areas immediately adjacent to the electrode. These electrodes could be used for long-term implantation in animals (up to 2 years). Clark, however, declined to state his results in calibrated units, preferring to report his data in the actual microampere currents that were measured, with the reasoning that determining the relation between the oxygen tension and the oxygen "activity" was not easily done. He did show that tissue oxygen could be increased by ventilation with 100% oxygen and decreased with hypoxic gas mixtures.

Clark described the mean oxygen availability (aO_2) and that it increased about twofold when pure oxygen was breathed, with a proportionate increase in the amplitude of the waves. Oxygen/nitrogen mixtures with O_2 between 0 and 20% showed a linear relation between aO_2 and pO_2. Oxygen concentrations between 20 and 100% produced a saturation effect that resulted in slope decreases. Administration of pure nitrogen caused an immediate decrease to near zero, which usually increased above baseline for $\geq$5 min after the readmission of air due to a hyperemic overshoot, which is the increase of cerebral circulation that follows hypoxia or short periods of anoxia. Exposure to a 5% CO_2/95% O_2 mix caused a significant increase in brain tissue pO_2 (up to threefold) over that resulting from inspiring pure oxygen. This effect was even more pronounced with higher CO_2 concentrations, such as 10 and 14%. After exposure to higher concentrations of CO_2, the aO_2 was slow in returning to baseline levels. Only slight alterations were observed with certain pharmacologic agents, such as anesthetics and pressor agents, but these responses appeared to parallel changes in CO_2 tension.

Clark also examined other species and made comparisons. Dog, guinea pig, and rat brain had very similar aO_2 to that of the cat.

Hyperventilation sufficient to reduce blood CO_2 and increase blood pH caused a decrease in mean aO_2. Hyperventilation with

oxygen (blood pH 7.85) reduced the aO_2, but hyperventilation with 5% CO_2/95% O_2 (pH 7.43) increased the aO_2 above baseline values (normal oxygen).

Smaller electrodes usually have shorter response times because of a shorter diffusion path. Electrodes with thick membranes may have response times of several minutes, but this can be of benefit when stability is necessary in environments where oxygen changes occur slowly. By the end of the 1950s, the Beckman Instrument Company developed a miniaturized Clark-type electrode (the size of a 20 g needle) and amplifier (Beckman/Spinco model 160), which could be used for *in vivo* preparations. Sugioka and Davis (92) applied it to the pentobarbital-anesthetized dog cerebral cortex and reported normal tissue pO_2 values of 8–20 torr. They also confirmed the observation that hyperventilation caused decreases in tissue pO_2.

Ingvar *et al.* (1960), using "Clark type" recessed electrodes, observed that naked electrodes tend to be unstable because of the changing catalytic activity of the platinum surface (11, 29). In these experiments, they studied the influence of hypoxia and hyperoxia on oxygen tension in the cortical surface of the cat brain. It was found that, depending on the preceding state of oxygen supply, oxygen breathing leads to different effects on the cortical pO_2 levels. In posthypoxic hyperoxia, the cortical pO_2 levels reached much higher levels than in ordinary hyperoxia (2–3 times higher). The difference was explained as being due to "reactive hyperemia." This group also showed, by experimentation and calculation, that the surface pO_2 recorded by such large electrodes (4-mm-diameter active area) did not reflect average tissue pO_2, but was closer to venous oxygen tension in the anesthetized dog (25).

In 1962, Cross and Silver (13) conducted an extensive study that examined oxygen tensions in various regions of the lightly anesthetized cat brain. These were the first investigators to use 1-μm glass-enclosed coated electrodes that were capable of making accurate local pO_2 measurements. An extensive description of the electrode construction and calibration has been provided (90). They observed an average oxygen tension level of 13 torr in grey matter, with lower levels recorded in white matter and higher levels in cerebral ventricles. The range of oxygen tensions recorded in the cortex was 10–30 torr. Minor and major variations of this tension were seen as the electrode moved down from the cortical surface. The changes in oxygen tensions were reproducible by reversing the progression and raising the electrode back up the same track.

The authors observed fairly high values for other subcortical regions but very low tensions in white matter, such as ventral medullary lamina of the thalamus ($<$1 torr). Sections were examined from the forebrains of rabbits that had been injected with India ink, which confirmed that the large white-matter tracts were poorly vascularized. The cortex and subcortical nuclei displayed a much greater, although variable density of capillaries (13).

In addition to oxygen-tension changes associated with different regions, many minor fluctuations were also recorded in localized areas (intervals of 10–50 μm) that could not be totally explained or accounted for through anatomic reconstructions. The fluctuations were reproducible and at times were as high as fourfold. The authors noted that this was potentially due to the tip of the electrode grazing small blood vessels as it passed through the tissue.

The greatest increases in oxygen tension were usually in sites where initial tension was high (*e.g.*, cortex, ventricles, diencephalon). Sites of low tension (white matter) had smaller increases. Regions with relatively high resting oxygen tension also showed greater decreases when hypoxic mixtures were inhaled (mixtures of nitrogen/nitrous oxide). Twenty seconds of nitrogen/nitrous exposure reduced oxygen tension to almost zero, and these reductions in oxygen tensions were usually followed by an overshoot when room air was restored.

Cross and Silver (13) also showed that hypercapnia (80% CO_2, 20% O_2) resulted in an increase in oxygen tension that usually exceeded the response after breathing pure oxygen. This was dependent on oxygen being in the mixture, because when pure CO_2 was inhaled, a decrease in oxygen tension was observed (anoxic conditions). In other organs, such as skin, hypercapnia produces vasoconstriction and subsequent decrease in pO_2.

Intravenous administration of 1–10 μg of adrenaline increased oxygen tension in the forebrain (by 20%) and reduced tension in the skin, testis, and mammary gland. The effect lasted 2–3 times longer in the periphery than in the brain. Electrical stimulation of the lateral or posterior hypothalamus, known to activate the adrenal medulla, produced similar increases in oxygen tension in the forebrain and reduction in the other organs. Section of the cervical sympathetic nerves did not affect basal oxygen tension in the forebrain, but nerve stimulation produced an ipsilateral reduction in forebrain oxygen tension ($\leq$50%), attributed to sympathetic-induced vasoconstriction.

Metzger (64) also used polarographic microelectrode measurements to examine the time course of pO_2 transients in the frontal and occipital cortices of the rat after abrupt changes of inspiratory O_2 and CO_2 concentration. The microelectrode measurements obtained confirmed results based on blood-gas data. The oxygen tension recorded during normoxia supported previous studies with values $<$20 torr (range, 10–20). The study showed that hypercapnia resulted in an increase in oxygen tension in all locations, whereas hyperoxia caused increased tissue pO_2 only near the arterial ends of capillaries. Their results also confirmed findings of previous studies that hypercapnia is more effective in increasing tissue pO_2 in the brain than is hyperoxia. They also suggested that tissue pO_2 fluctuation (or oscillation) after severe hypoxia represents the delayed vasoconstriction of brain vessels.

Nair *et al.* (66) used smaller microelectrodes than previous microelectrode studies to observe oxygen tensions in the cerebral cortex of anesthetized and artificially ventilated cats. They observed $>$600 different locations with an oxygen-tension range from 0 to 99 mm Hg and a mean value of 38.7 $\pm$ 0.93 (SEM) torr. Interindividual variation in the mean pO_2 ranged from 18.8 to 60.4 among the various numbers of locations. Under anoxic conditions, tissue pO_2 decreased to zero in most of the 45 locations tested (30 of 45). In four of the 45 measurements, pO_2 decreased to 1–3 mm Hg. Of the remaining 11 measurements in which the pO_2 value did not go down to zero or close to it, seven were from one cat that was relatively hypothermic. In two of the cats (two of nine), tissue pO_2 during N_2 breathing remained above zero (as high as 27 mm Hg in one trial) in eight of the 10 locations tested. The authors had no explanation for these observations. When the animals were returned to room air, the pO_2 generally displayed an overshoot

before returning to the control value. Ventilation with 100% O_2 caused an increase in tissue pO_2 in 22 of 29 locations, and when room air was returned, values returned to control values in a few minutes. The higher the initial control pO_2, the greater the increase in pO_2 during the hyperoxic event. The authors concluded that the high pO_2 and increased responsiveness were potentially due to close proximity of the microelectrode to blood vessels. This result could have also been due to higher microvascular density. They also concluded that the variation from the norm in the other seven was due to the "vasoconstrictive action of oxygen on the vessels."

Leniger-Follert *et al.* (48) observed local tissue oxygen pressure at adjacent sites of the cat cerebral cortex with a platinum multiwire surface electrode. Measurements were made under steady-state conditions and with different arterial oxygen supply. Under normoxic and steady-state conditions, tissue oxygen measurements were made that varied from 0 torr to levels close to arterial pO_2. Under normoxic conditions, different tissue pO_2 values at adjacent sites were expected because of the diffusive transport of oxygen, causing an oxygen-pressure field in the tissue. The authors also noticed rhythmic variations in pO_2, as did previous studies. Adjacent recording sites (within 350–600 μm apart) responded very differently to increased arterial oxygen supply. The responses ranged from linear responses on par with arterial pO_2 to small increases and decreases (constant values were also recorded). It was concluded that these local differences were due to local regulation of microflow, but differences in oxygen consumption could not be excluded. This local regulation of pO_2 was eliminated by adding CO_2 to the gas mixture or by producing tissue anoxia. In these cases, local pO_2 decreased to hypoxic or anoxic levels at all sites measured.

Mild (in retrospect) controversies occupied the experimentalists of the early 1970s. The controversies centered around calibration-accuracy issues, physiologic and instrumental response times, and as has been alluded to, whether nitrogen-induced anoxia resulted in a decrease to zero in cerebral cortical pO_2 or whether some residual tissue oxygen could remain (*i.e.*, that oxygen consumption ceased before tissue oxygen was completely gone). In contrast to the preceding studies, Bicher *et al.* (5, 6) reported that respiration with nitrogen reduced tissue pO_2 slightly after a 30-s latency period, which then remained relatively constant despite a very low, near-zero arterial O_2. One key difference between the studies is the fact that the recordings of Bicher *et al.* were made with needle electrodes from deep layers of the cat cortex, whereas other groups usually recorded from layers closer to or at the surface.

The weight of the evidence produced from these early studies is clearly supportive of the conclusion that tissue pO_2 is lower than venous pO_2 and that changes in tissue oxygen concentration reflect changes in blood-oxygen content and brain blood flow in a predictable and consistent manner.

Sick and Kreisman (37, 88) used coated, glass-enclosed platinum microelecrodes with integral reference electrodes, and with the added innovation of a feedback-controlled polarization circuit that effectively controlled changes in intrinsic brain electrical-potential changes as a result of neuronal activity. This was important because the microelectrodes used in brain-tissue studies have no real plateau region in the I-V curve, so even small changes in voltage could result in non–oxygen-dependent changes in current. Using these microelectrodes, we confirmed, in the anesthetized rat cerebral cortex, the dependence of tissue pO_2 on oxygen availability (38, 89). We also demonstrated that increasing local blood flow with the carbonic anhydrase inhibitor, acetazolamide, transiently increased cortical pO_2 (42). The results are demonstrated in Fig. 1. The figure shows the response of four individual rats, anesthetized with chloral hydrate, to intravenous administration of acetazolamide, 50 mg/kg. Note the spread of starting pO_2 in the rats and the differences in magnitude of the responses. This dose of acetazolamide resulted in doubling of the cerebral blood flow, lasting >1 h, as demonstrated in a parallel series of rats studied at the same time (42).

Contamination of the electrode surface has long been recognized as a major source of potential error in quantitation of the oxygen signal. Some attempts have been made to protect the active surface of the electrode from the tissue without restricting access to tissue oxygen. One interesting approach was to use a perforated capsule, with a Beckman/Spinco electrode system, that was permanently implanted into the brain and was invaded by the tissue and vascularized over a 4-week period (32). These investigators reported oxygen partial pressures of 15.8 $\pm$ 1.0 torr in the parietal cortex of five pentobarbital-anesthetized dogs. A more recent attempt was made by Prohaska *et al.* (75, 76), who designed an electrode using thin film technology in which the dimensions and polarization of the electrode were controlled by virtue of a box structure over the surface. Voltage and temperature sensors were included on the substrate. In our hands, these electrodes provided data consistent with the previous literature (43, 44).

Other limitations of O_2 electrodes must also be taken into account. First, the consumption of oxygen has the potential to alter the local environment, which can be very important when making measurements with small samples. Differences between probes and performance change with time, and, therefore, calibration is needed often. Some electrodes cannot be calibrated properly for use in tissue; thus, they can provide only qualitative data (so the term "oxygen availability" has been used also to describe changes in relative oxygen tension). Oxygen probes are subject to electromagnetic interference from radiofrequency signals, alternating line currents, capacitance effects, *etc*. Some electrodes can be affected by certain substances like nitrous ox-

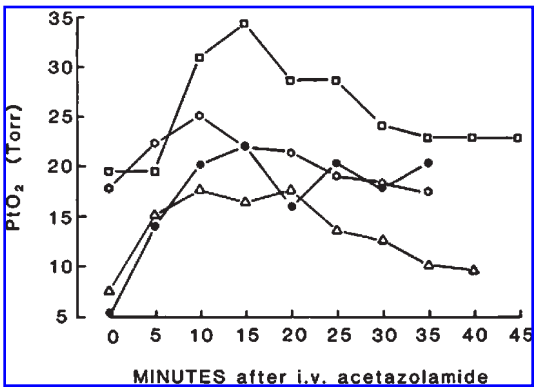

FIG. 1. Effect of acetazolamide (50 mg/kg, i.v.) on brain-tissue oxygen tension in four anesthetized rats. Previously unpublished data taken from (42).

ide and halogenated anesthetic gases (84). Persistently high pO_2 and a lack of responsiveness of the electrode to changes in circulating blood oxygenation may indicate the presence of a small hematoma in long-term implantation models (97). Electrodes are also spatially limited, so to measure a distribution, multiple probe assemblies for simultaneous measurement (48) or multiple sequential electrode repositionings (89) or both would be required.

Summary. The polarographic method is responsible for most of the quantitative measurements of brain oxygen tension *in vivo*. Over the past 50-year period, the method has established a number of major findings, among which are the observations that brain-tissue oxygen partial pressures are less than venous pO_2, and that the brain-tissue oxygen pressures are dependent on arterial pO_2 and cerebral blood flow. The method has been well worked out, and the sources of error are fairly well known. Two disadvantages include the electrode providing only point measurements and invasiveness, in that it is difficult to use in the nonanesthetized state. The method is being superseded by optical and EPR methods, primarily because of the ability of these techniques to provide images.

OPTICAL TECHNIQUES

The optical methods of oxygen detection are based on the property of oxygen to participate or facilitate in the transition from higher-energy states of optically active molecules to lower-energy states, thus interfering with or quenching the fluorescent or phosphorescent emission of photons in an oxygen concentration–dependent manner (33). The relation between the oxygen concentration and fluorescence/phosphorescence signal from the indicator is given by the Stern-Vollmer equation:

$$I = I_0/(1 + K \cdot pO_2)$$

where I_0 is the fluorescent intensity in the absence of oxygen, I is the fluorescence at any given O_2 concentration, and K is the quenching coefficient. The quenching constant can be further described by

$$K = k+ \cdot \alpha O_2 \cdot \tau_0$$

where k+ is the collisional constant, αO_2 is the oxygen solubility coefficient, and τ_0 is the mean lifetime of the excited state at zero oxygen. The relation holds for lifetime as well as intensity (97).

Fluorescence

Mitnick and Jobsis (65) used the fluorescent probe, pyrene butyric acid (PBA), to measure the pO_2 from the surface of the cat brain (65), reporting a fairly high mean level >40 torr. The probe was given intravenously and penetrated the tissue parenchyma. The cats were prepared as *cerveau isole* preparations, and the fluorescence signal was recorded from a 3.2-mm-diameter field on the cerebral cortex.

The applicability of PBA to biologic systems was first reported by Vaughan and Weber (99), who showed that PBA could be excited with near-ultraviolet irradiation to produce a fluorescence emission that was shown to be quenched by oxygen over a 0- to 500-mm Hg pO_2 range. Knopp and Longmuir (36) demonstrated that PBA quickly entered cells, in this case liver cells, and did not cause any noticeable decline in oxygen consumption (36). Some advantages of using PBA include the fluorochrome being nontoxic, noninvasive, and non–oxygen consumptive. Correction for hemoglobin absorption in the optical field was made by subtraction of the reflected excitation light signal (340 nm) from the emitted fluorescence signal (397 nm).

Lubbers (60, 72) used PBA in the design of an "optode" for *in vivo* measurements of tissue oxygen tension. These optodes had obvious advantages over the systemic administration of the indicator in terms of toxicity, stability, and localization. These optodes were also considered superior to polarographic electrodes in the sense that they do not have the signal distortions due to a remote reference electrode, they do not alter the oxygen pressure field by consuming oxygen, and they are more stable in the tissue environment. These probes, however, are rather large compared with the smallest polarographic electrodes and thus do not have the same spatial-resolution capability.

Luminescence/phosphoresence

Luminescent material can be placed in a plastic oxygen-permeable material or trapped at the bottom end of an optical fiber to make useful optodes. The most commonly used and studied compounds in optodes are based on ruthenium red. The ruthenium molecules absorb photons of light, and the electrons are energized, moving from the ground state to an excited singlet state. The commercially available Oxylite system (Oxford Optronics, Ltd., Oxford, England) is a current method available for use to measure brain oxygen tensions.

Nwaigwe *et al*. (67) used the Oxylite probe to compare tissue pO_2 in thalamus and hypothalamus, reporting mean levels of just under 30 torr in the thalamus and much lower levels, <10 torr, in the hypothalamus (67). The probe was 250 μm in diameter, and temperature sensitive (~1 torr/°C).

Wilson *et al.* (103), using the porphyrin phosphorescence–based method described by Rumsey *et al*. (83), reported cerebral cortical pO_2 levels of ~20 torr in newborn piglets under fentanyl and nitrous oxide. In another study, they reported a mean pO_2 of ~32 torr (93). The probe used in the study was designed to remain in the vasculature. This method would seem to be ideal for reporting the oxygen distribution in the cerebral cortex, but these investigators have not yet done this, only reporting mean values for cortical oxygen.

Summary. Fluorescence is not being pursued, mainly because the intensity measurement is subject to interference by hemoglobin saturation and volume changes. Measuring the decay time would help this, but it is very fast for fluorescence and phosphorescence, which may present another problem. Phosphorescence currently involves just the vascular space, but permeable indicators are possible and may be in development. The ability to visualize the parenchymal spatial distribution is a powerful asset, but has not yet been exploited.

EPR OXIMETRY

Electron paramagnetic resonance, or EPR (also known as electron spin resonance, ESR), is another method that has been adapted for measuring brain oxygen tension *in vivo* (18, 51). This method measures oxygen by examining its effect on a spin probe, most commonly lithium phthalocyanine (LiPc) (18), using an EPR spectrometer adapted for *in vivo* use. One or more LiPc crystals are inserted into the brain of the animal subject a few days before the study. The crystals are essentially inert and do not cause damage or an injury response. Measurements from multiple sites can be made by adding a field gradient (18), allowing as many as 35 different measurements from a single 1-cm-diameter sphere of tissue (27). The animal can be studied under awake or anesthetized conditions, and multiple measurements spread over many days can be made. LiPc crystals are highly sensitive at low PtO_2 tensions, respond rapidly, have stable calibration, and are not affected by changes in pH or redox conditions (51, 80). Recordings made with EPR oximetry are from deeper locations in the cortex than those assayed by surface fluorescence/phosphorescence. Brain-tissue oxygen tension measured with this method has been reported between 25 torr (17) and 35 torr (50) in the awake rat.

EPR oximetry can also be carried out with the use of soluble materials such as nitroxides, which can be designed to target specific environments and compartments within a cell (97). These soluble materials can supply signals over large regions, but the probe is lost rapidly in the body (97). These soluble probes can be used for imaging (54), but the temporal and spatial resolution is still crude.

Summary

EPR methods have great promise for accurate, reproducible, and noninvasive measurement of brain oxygen. Current spatial resolution is not able to resolve functional units.

MASS SPECTROMETRY

Molecular oxygen can be identified and measured quantitatively by mass spectrometry. In 1969, Owens *et al*. (73) adapted a mass spectrometry probe used for blood-gas analysis for use in brain. They inserted a Teflon-tipped 1-cm-long, 1-mm-diameter cannula into the cerebral hemisphere of dogs under pentobarbital anesthesia. The cannula was attached to a mass spectrometer *via* a copper tube. This method was used in a series of human patients undergoing neurosurgical procedures, and cerebral cortical tissue pO_2 was reported to range between 12 and 49 torr (79).

Seylaz *et al.* (86, 87) developed a mass spectrograph technique for *in vivo* measurement of physiologic gas partial pressures in local regions of the rabbit brain. This technique consists of sampling and analyzing certain quantities of gas in the medium under study. In the past, difficulties arose in the development of miniature sampling cannulas for minimal interruption of gas equilibrium during the actual withdrawal. They reported being able to obtain simultaneous, continuous, and local measurements of blood flow and physiologic gas partial pressures using a single probe permanently implanted in deep-brain structures. The purpose of this was to obtain more precise information on the metabolic mechanisms involved in the regulation of the cerebral circulation. The authors mention the fact that cerebral oxygen tension is dependent on both vascular and metabolic states, so continuous measurement of pO_2 provides assurance that a steady state exists during the period of CBF determination. In these studies, the mean partial pressure of oxygen was 16.9 ± 1.6 mm Hg (SEM) in the caudate nucleus of 13 rabbits. Variability existed between the 13 rabbits, with values ranging from 6.3 to 26.0 mm Hg. These probes were calibrated *in vitro* before permanent implantation into the brain. Measurements were carried out for $\geq$2 weeks after implantation to allow resorption of any edema or inflammation or both that may have occurred.

Summary

The invasiveness and the time response make mass spectrometry less attractive as a method, especially in the face of better options.

QUALITATIVE METHODS

NMR/MRI

Fiat *et al*. (23, 74) conducted an *in vivo* ^{17}O NMR study to observe the cerebral $H_2{}^{17}O$ concentration during inhalation of $^{17}O_2$. This was done after a similar *in vitro* study showed that oxygen-17 could be used as a tracer in the study of cerebral oxygen utilization. The study used ^{17}O-NMR spectroscopy to detect metabolic water produced in rats after administration of oxygen-17. This technique has been recently reviewed (105). Like PET, this technique may be more useful for measurement of $CMRO_2$ rather than the oxygen tension itself. Thus, they provide information from the utilization side of the ledger rather than the supply side.

^1H-NMR was also used to show that *in vivo* changes occurred in image intensity in the brains of rats that inhaled oxygen-17 gas (2). Because water is the predominant end product of the metabolism of oxygen in the brain, this approach has been used to measure cerebral oxygen consumption ($CMRO_2$).

The average values of cortical CBF and $CMRO_2$ for four control rats were calculated using the Kety-Schmidt approach and were 1.4 ± 0.5 ml/min/g and 3.6 ± 0.4 mmol/min/kg brain, respectively. They observed that the brain $H_2{}^{17}O$ concentration surpassed the predicted concentration from cerebral metabolism and did not plateau after 10 min of breathing $^{17}O_2$. The explanation was that most of this increase is primarily due to recirculation from other bodily organs, rather than direct oxygen metabolism in the brain.

NMR has been used with perfluorocarbons to measure pO_2, and maps have been made (20). The pO_2 of the emulsion is very high, so this is not useful as a quantitative tissue-oxygen indicator. The resultant histogram is more bell-shaped and centered $\sim$250 torr. A modification with injected perfluorocarbon directly into the tissue has been done (19).

In vivo changes in blood oxygenation could be detected with MRI, first in rats (70), and then in humans (41, 71). The MRI

signal became known as the blood-oxygen-level–dependent or BOLD signal. Human studies showing BOLD signal changes led to the development of *f*MRI. When a BOLD signal is observed/generated, blood flow to that particular region of the brain has changed out of proportion to the adjustment in oxygen consumption (34, 35). When blood flow changes more than oxygen consumption (in either direction), a mutual change is noted in the amount of deoxyhemoglobin present locally in the tissue, changing the local magnetic field properties. In general, the method for detection involves MRI with pulse sequences that are very responsive to the paramagnetism related to the deoxy state of hemoglobin (77, 78).

Summary. The BOLD *f*MRI method has much promise for human cognitive function studies, as well as for diagnosis and treatment assessment for cerebrovascular disease.

Positron emission tomography

Raichle (77) discussed functional brain imaging by PET and MRI. PET detects ^{15}O (94, 95). Like ^{18}O mass spectrometry studies (26), PET detection of ^{15}O can be used to calculate oxygen consumption, but not pO_2.

Optical methods: in vivo *optical spectroscopy*

The color shifts that hemoglobin undergoes in the presence of oxygen have been used to measure hemoglobin saturation and, with a calibrated hemoglobin/oxygen saturation curve, can be used to estimate the pO_2 of blood. Changes in hemoglobin saturation in the cerebral cortical capillary bed in response to changes in FiO_2 and CO_2 were made in the visible spectrum with a reflectance spectrophotometer from the surface of cat, rabbit, and rat brain (31, 49, 82), but these were qualitative studies. Imaging of hemoglobin as an intrinsic signal has also been useful (24).

When Jobsis (30) introduced the near infrared spectroscopy (NIRS) method in 1977, it soon became possible to make more quantitative estimates of tissue hemoglobin saturation (8, 16, 22). The NIRS technique is becoming more popular and is in use clinically (62). As an imaging method, NIRS provides an alternate to BOLD studies in attempts to understand better the dynamic brain metabolic and vascular responses (68, 100, 101). Despite the theoretic possibility for estimating pO_2 from the hemoglobin saturation, it has not yet been done.

Summary. NMR, PET, and NIRS are mostly qualitative methods for oxygen measurement. They do not directly give useful descriptions of oxygen availability, but they are useful for dynamic measurements because they have reasonable temporal resolution, and repeated measurements can be made.

SPATIAL DISTRIBUTION OF OXYGEN IN THE BRAIN: pO_2 HISTOGRAM

Early studies of brain oxygen noted that the oxygen tension in the tissue varied within small distances and that most of the measured tensions were low. Davies and Bronk (15) reported an oxygen profile across the surface of the cat cortex using a 14-μm-diameter open-type polarographic electrode. In the 1960s, it was abundantly clear that oxygen was distributed heterogeneously in the mammalian brain (on a microregional level). The usual interpretation for oxygen steep gradients invoked distance from the capillary supply as the likely explanation (15, 90). Lubbers (57) pointed out a number of important observations concerning the oxygen field in the brain. These are nicely summarized in the 1969 paper presented at the International Symposium on Oxygen Pressure Recording, held in Nijmegen in 1968. He stated, based on Krogh concepts (39) as developed for the brain by Thews (96), that the tissue oxygen tension at any given locus depended on the oxygen tension at the nearest capillary wall, the local tissue respiration, the diffusion coefficient for oxygen in the tissue, and the distance from the capillary. The oxygen-diffusion flux caused by the tissue-respiration variations would produce large local differences in oxygen tension. Thus, he pointed out, no "characteristic tissue oxygen tension" or representative average oxygen tension exists, but an oxygen-tension field is present in the tissue. The oxygen supply to the tissue can best be characterized by a pO_2 distribution curve. Investigators who recorded enough systematic observations to construct a meaningful frequency histogram noted that the distribution was left-shifted, the shape reminiscent of a log normal distribution (12, 58, 59, 66, 85, 89, 91). About two thirds of the measurements are less than the mean value (91). Thus, the mean value cannot be a good representation of the tissue oxygen field or of oxygen supply to the tissue. This obvious conclusion is continually ignored in the current literature, where discussions of the average brain pO_2 continue.

The only good, quantitative measurements of the oxygen field so far have come from microelectrode studies. This is be-

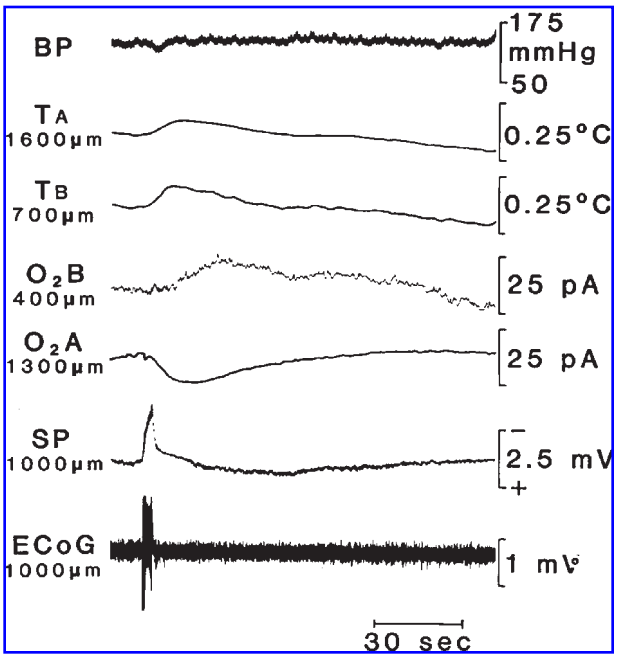

FIG. 2. The effect of 5 s of direct cortical electrical stimulation on tissue oxygen tension and temperature at multiple depths below the cerebral parietal cortical surface. Reprinted with permission from (44).

cause the average intercapillary distance in brain is ~50–60 μm (4). It has been estimated that the oxygen-sensing field of polarographic microelectrodes is about π times the diameter (58), so an electrode with a diameter of closer to 1 μm is suitable, but one with 10-μm diameter would not be.

Oxygen-distribution curves have been recorded for cat (66), rabbit (91), baboon (12), rat (85, 89), and guinea pig (7, 59). These all have about the same distribution under resting conditions and anesthesia, suggesting a common mammalian trait. Qualitative and quantitative differences in regional oxygen distribution were found between the rat and turtle brains at rest and in response to changes of inspired oxygen concentration (89). Sick *et al.* (89) found that the average oxygen tensions were similar, with values of 12.9 ± 0.9 (n = 136) and 12.5 ± 1.3 (n = 73) in the rat and turtle brain, respectively (89). The peak frequency in both species was ~10 mm Hg, but the distribution of oxygen in the rat brain appeared to be left-shifted, whereas that of the turtle appeared to be more normally distributed (89). Interestingly, in the rat brain, a higher number of observations of tissue pO_2 >20 mm Hg, 31 of 136, were found versus the turtle brain, three of 73 (89). These differences in O_2 profile may be due to higher O_2 consumption and greater cerebral blood flow in the rat brain (89).

Nair *et al*. (66) reported individual pO_2 histograms for nine

TABLE 1. QUANTITATIVE ESTIMATES OF BRAIN TISSUE pO_2 PARTIAL PRESSURE BY DIFFERENT TECHNIQUES AND UNDER VARIOUS CONDITIONS

PtO_2 values	*Method*	*Species*	*Status*	*Citation*
33 ± 11	Polarographic	Human	Anesthetized	Charbel, 1997 (9)
2.0–10	Polarographic	Cat	Anesthetized	Davies & Bronk, 1957 (15)
10.0–30	Polarographic	Cat	Urethane (20% sol, 1 g/kg)	Cross & Silver, 1962 (13)
10.0–20	Polarographic	Rat	Na-pentobarbital (40 mg/kg)	Metzger, 1971 (64)
0–99 (avg, 38.7 ± 0.9)	Polarographic	Cat	Na-pentobarbital (30–40 mg/kg)	Nair, 1975 (66)
0–90 (freq max 25–30)	Polarographic	Cat	Pentobarbital (25–30 mg/kg), gallaminetriethiodine (paralytic, 10 mg/kg)	Leniger-Follert, 1975 (48)
12.9 ± 0.9	Polarographic	Rat	Na-pentobarbital (35 mg/kg), D-Tubocurarine hydrochloride (10 mg/kg)	Sick, 1982 (89)
12.5 ± 1.3	Polarographic	Turtle	Na-pentobarbital (35 mg/kg), D-Tubocurarine hydrochloride (10 mg/kg)	Sick, 1982 (89)
23.3	Polarographic	G. Pig	Anesthetized	Lubbers & Baumgarti, 1997 (59)
29 ± 5	Polarographic	Rat	Control, brief isoflurane (2%), pancuronium bromide (1 mg/kg)	Seyde & Longnecker, 1986 (85)
35 ± 7	Polarographic	Rat	Isoflurane (4%), pancuronium bromide (1 mg/kg)	Seyde & Longnecker, 1986 (85)
22 ± 5	Polarographic	Rat	Sodium nitroprusside (3.8 mg/kg), pancuronium bromide (1 mg/kg)	Seyde & Longnecker, 1986 (85)
13 ± 5	Polarographic	Rat	2-Chloroadenosine (0.8 mg/kg), pancuronium bromide (1 mg/kg)	Seyde & Longnecker, 1986 (85)
1–79 (avg, 23.8 ± 12)	Polarographic	Baboon	Anesthetized	Crockard, 1976 (12)
16–59 (avg, 29.8)	Polarographic	Human	Anesthetized	Baker, 1975 (3)
0–90 (avg, 25)	Polarographic	Cat	Na-pentobarbital (30–40 mg/kg)	Whalen, 1970 (102)
24.5 ± 18	Polarographic	Rabbit	Urethane (20% sol, 1 g/kg)	Smith, 1977 (91)
18.4 ± 1.2	Polarographic	G. Pig	Na-pentobarbital (30–40 mg/kg)	Buerk & Nair, 1993 (7)
28–32 (hypothalamus)	Optical (ruthenium)	Rat	Isoflurane (1%)	Nwaigwe, 2003 (67)
10–15 (thalamus)	Optical (ruthenium)	Rat	Isoflurane (1%)	Nwaigwe, 2003 (67)
32.3 ± 0.8 (22% O_2)	Optical (Phos)	Pig	Halothane (3–4%)	Tammela, 1996 (93)
25–35	Optical (Phos)	Pig	Halothane, analgesic, tubocurarine	Wilson, 1991 (103)
42.8 ± 8.6	Optical (Fluor, PBA)	Cat	Ether, *cerveau isole*	Mitnick & Jobsis, 1976 (65)

(*Continued*)

TABLE 1. QUANTITATIVE ESTIMATES OF BRAIN TISSUE pO_2 PARTIAL PRESSURE BY DIFFERENT TECHNIQUES AND UNDER VARIOUS CONDITIONS (CONT'D)

PtO_2 values	*Method*	*Species*	*Status*	*Citation*
12.0–49	Mass spectrometry	Human	Anesthetized	Roberts & Owens, 1972 (79)
16.9 ± 1.6	Mass spectrometry	Rabbit	Anesthetized	Seylaz, 1978 (86)
9.0 ± 2.1	EPR (LiPC)	Rat	Pentobarbital	Hou, 2003 (28)
13.0 ± 2.9	EPR (LiPC)	Rat	Chloralose/Urethane	Hou, 2003 (28)
16.5 ± 0.8	EPR (LiPC)	Rat	Halothane	Hou, 2003 (28)
38.0 ± 4.5	EPR (LiPC)	Rat	Isoflurane	Hou, 2003 (28)
3.5 ± 0.3	EPR (LiPC)	Rat	Ketamine/Xylazine	Hou, 2003 (28)
15.1 ± 1.8 (30% O_2)	EPR (LiPC)	Rat	Ketamine (8–10 mg/100 g), Xylazine (1.1–1.4 mg/100 g)	Rolett, 2000 (80)
55	EPR (LiPC)	Rat	Awake	Liu, 1993 (51)
45–50	EPR (LiPC)	Rat	Ketamine	Liu, 1993 (51)
20	EPR (LiPC)	Rat	Nembutal	Liu, 1993 (51)
34.1 ± 3.2	EPR (LiPC)	Rat	Awake	Liu, 1995 (50)
20–30	EPR (LiPC)	Rat	Isoflurane (1%)	Liu, 1995 (50)
12.0–20	EPR (LiPC)	Rat	Ketamine/Xylazine (100/10 mg/kg)	Liu, 1995 (50)
10.0–20	EPR (LiPC)	Rat	Pentobarbital (50 mg/kg)	Liu, 1995 (50)
26.5 ± 11	EPR (LiPC)	Rat	Awake	Dunn, 2000 (17)
26.6 ± 7.0	EPR (LiPC)	Rat	Isoflurane (1%)	Lei, 2001 (46)
30–35	EPR (LiPC)	Rat	Isoflurane (4%)	Liu, 2004 (54)
31–36	EPR (LiPC)	Rat	Isoflurane (1.75%) in 705 Nitrous	Liu, 2006 (52)
33.4 ± 6	EPR (LiPc)	Rat	Isoflurane (4%)	Liu, 2004 (53)

experimental cats, and from these, the mean pO_2 for the cats was created (66). The mean pO_2 for each cat did not correlate with arterial pressure, pO_2, pH, or body temperature. The recorded pO_2 values depended on the depth at which the measurement was made. On average, a linear decrease in pO_2 was found from the surface of the cortex (just <70 mm Hg on average) to a depth of 500–600 μm (just <35–40 mm Hg). From 700 to 1,600 μm, pO_2 remained in the range of 25–35 mm Hg. Where investigators report a relation between depth in the cortex and tissue oxygen tension, the relation is always that of decreasing pO_2 with depth (13, 21, 102). Other investigators did not observe a change in oxygen tension with depth through the cortex (59, 90). Whether or not a surface covering makes a large difference when recording and interpreting the data (21) is not known. White matter has been consistently shown to have lower oxygen tensions, as have subcortical structures such as the hippocampus (13, 21).

Summary

Oxygen is heterogeneously distributed on a microregional level and responds to increases and decreases in local availability and local metabolism. Many low levels of oxygen mean that the environment is low oxygen.

TEMPORAL DISTRIBUTION OF O_2: DYNAMIC ACTIVATION STUDIES

The development of the BOLD *f*MRI method (70) and its application to human studies of cognition (41, 71) has given new perspective and significance to studies of transient functional activation. The BOLD signal in response to transient focal brain activation is under intense scrutiny, and the current state of understanding this has been recently reviewed (78). Some useful insights can be gleaned from the oxygen-measurement literature over the past 50 years. Brief activations of cortical neurons result in negative steady potential shifts on the order of a few millivolts that are accompanied by an increase in extracellular potassium ions of up to a few millimolar (55, 61). The increased work stimulated by the increased neuronal activity produces an increase in oxidative metabolism that persists for many seconds beyond the electrical and ionic transient. Such transient metabolic responses have been observed by measurement of NADH/NAD+ redox changes by surface fluorescence methods (55, 81). Measurements of hemoglobin saturation by optical methods have, for the most part, echoed the BOLD data, with the consensus being that a small "initial dip" toward disoxygenation occurs, followed by an arteriolarization of the local capillary bed, resulting in a large shift to oxygenated hemoglobin (24, 31). Direct measurements of tissue oxygen have been more varied. The first observations were reported by Leniger-Follert *et al*. (47). In that study, they simultaneously measured microflow and local pO_2 to examine the kinetics of microflow and its dependence on local pO_2 during electrical stimulation of the cortex in cats (47). During local cortical stimulation, the arterial blood pressure remained constant. The reaction pattern of the microflow in response to electrical stimulation was uniform at all sites measured. An increase in microflow was seen within 1–2 s after beginning stimulation, and this reached a maximal hyperemia after the end of stimulation. The increase in microflow and maximum of hyperemia

produced depended on the duration and amplitude of stimulus. The return of microflow to baseline levels took ≥30 s and up to several minutes, depending on the intensity of stimulation. Usually no undershoot of microflow occurred on return to initial levels. No "dip" in tissue pO_2 was reported.

Metzger (63), conversely, reported that in most of the experiments conducted at normoxia, a continuous pO_2 decrease was seen in response to stimulation, which they interpreted as being due to increased oxygen consumption and consequent local hypoxia. The authors referred to a second group of experiments in a subset of rats in which increases and decreases in pO_2 were observed at different locations on the cortex. In a few experiments, the pia vessels were stimulated directly, producing an initial increase in pO_2 followed by a decrease.

Surface phosphorescence measurements of tissue oxygen tension during activation agreed closely with optically determined hemoglobin saturation, exhibiting a biphasic response (98). A similar response was observed in the cerebellum linked to microflow increases (69).

Our own study used reflection-difference spectra to demonstrate that cytochrome oxidase becomes more oxidized in response to direct cortical stimulation (45), confirming that a portion of the cytochrome oxidase pool was reduced when the brain was normoxic before stimulation. Tissue oxygen tension increased with a time course that tracked the vascular change. In a later study, we observed differential responses at different depths within the cortex (43, 44). When the cortex was stimulated, an oxygen electrode at a depth of 400 μm below the surface exhibited an increase in oxygen tension, whereas a simultaneous recording from 1,300 μm below the surface showed a decrease (see Fig. 2). These results suggest that layer-specific responses to activation in the cerebral cortex influence the measurement, perhaps in the profile of ions such as potassium (56) or heterogeneous distributions of cell types in the various layers or both. Thus, those techniques that have a more superficial source will display the concomitants of increased oxygen, and those methods that include the deeper layers may produce oxygen and hemoglobin dips. This might correspond to the activation depth profile indicated by K^+ ion–selective microelectrod (56).

Summary

Tissue oxygen tension can rapidly change when neuronal activity and capillary microflow are changed. This is the basis for the BOLD signal, and that fact means that a great need exists for quantitative measures with good spatial and temporal resolution (equal to BOLD). As a principle, it appears fairly robustly that the oxygen field is kept deliberately low under idling conditions and then is increased when the tissue is activated. Thus, the tissue lives usually under low oxygen, but briefly has bouts of high oxygen. Unit volumes and cortical columns appear to become activated together. This also seems to take place in the cerebellum, but we are uncertain about subcortical regions of the brain.

ACKNOWLEDGMENTS

This research has been supported by the National Institutes of Health, R01-NS38632 and P50 GM066309. Constantinos Tsipis, Xiaoyan Sun, Bernadette Erokwu, and Kui Xu contributed to the previously unpublished experiments, diagrams, and figures.

ABBREVIATIONS

BOLD, Blood oxygen level dependent; CBF, cerebral blood flow; CBV, cerebral blood volume; $CMRO_2$, cerebral metabolic rate of oxygen consumption; EPR, electron paramagnetic resonance; FiO_2, fraction of inspired oxygen; *f*MRI, functional MRI; Hb, hemoglobin; I-V, current–voltage (refers to curves used to calibrate electrodes); mm Hg, millimeter of mercury (atmospheric pressure); MR, magnetic resonance; MRI, magnetic resonance imaging; NAD^+, nicotinamide adenine dinucleotide; NADH, nicotinamide adenine dinucleotide (reduced form); NIRS, near-infrared spectroscopy; NMR, nuclear magnetic resonance; aO_2, mean oxygen availability; PET, positron emission tomography; pO_2, partial pressure of oxygen; torr, same as mm Hg.

REFERENCES

1. Acker T and Acker H. Cellular oxygen sensing need in CNS function: physiological and pathological implications. *J Exp Biol* 207: 3171–3188, 2004.
2. Arai T, Nakao S, Mori K, Ishimori K, Morishima I, Miyazawa T, and Fritz-Zieroth B. Cerebral oxygen utilization analyzed by the use of oxygen-17 and its nuclear magnetic resonance. *Biochem Biophys Res Commun* 169: 153–158, 1990.
3. Baker NA. A galvanic cell suitable for monitoring cortical oxygen in man. *Med Biol Eng* 13: 443–449, 1975.
4. Bar T. The vascular system of the cerebral cortex. *Adv Anat Embryol Cell Biol* 59: 1–62, 1980.
5. Bicher HI, Bruley D, Knisely MH, and Reneau DD. Effect of microcirculation changes on brain tissue oxygenation. *J Physiol (Lond)* 217: 689–707, 1971.
6. Bicher HI, Reneau DD, Bruley DF, and Knisely MH. Brain oxygen supply and neuronal activity under normal and hypoglycemic conditions. *Am J Physiol* 224: 275–282, 1973.
7. Buerk DG and Nair P. $PtiO_2$ and $CMRO_2$ changes in cortex and hippocampus of aging gerbil brain. *J Appl Physiol* 74: 1723–1728, 1993.
8. Chance B, Leigh JS, Miyake H, Smith DS, Nioka S, Greenfield R, Finander M, Kaufmann K, Levy W, Young M, Cohen P, Yoshioka H, and Boretsky R. Comparison of time-resolved and -unresolved measurements of deoxyhemoglobin in brain. *Proc Natl Acad Sci USA* 85: 4971–4975, 1988.
9. Charbel FT, Hoffman WE, Misra M, Hannigan K, and Ausman JI. Cerebral interstitial tissue oxygen tension, pH, HCO_3, CO_2. *Surg Neurol* 48: 414–417, 1997.
10. Clark LC Jr, Misrahy G, and Fox RP. Chronically implanted polarographic electrodes. *J Appl Physiol* 13: 85–89, 1958.
11. Connelly CM. Methods for measuring tissue oxygen tension; theory and evaluation: the oxygen electrode. *Fed Proc* 16: 681–684, 1957.
12. Crockard HA, Symon L, Branston NM, Juhasz J, and Wahid A. Measurements of oxygen tension in the cerebral cortex of baboons. *J Neurol Sci* 27: 17–28, 1976.
13. Cross BA and Silver IA. Some factors affecting oxygen tension in the brain and other organs. *Proc R Soc Lond B* 156: 483–499, 1962.
14. Davies PW and Brink FJ. Microelectrodes for measuring local oxygen tension in animal tissues. *Rev Sci Instrum* 13: 524–533, 1942.

15. Davies PW and Bronk DW. Oxygen tensions in mammalian brain. *Fed Proc* 16: 689–692, 1957.
16. Delpy DT, Cope M, van der Zee P, Arridge S, Wray S, and Wyatt J. Estimation of optical path length through tissue from direct time of flight measurement. *Phys Med Biol* 33: 1433–1442, 1988.
17. Dunn JF, Grinberg O, Roche M, Nwaigwe CI, Hou HG, and Swartz HM. Noninvasive assessment of cerebral oxygenation during acclimation to hypobaric hypoxia. *J Cereb Blood Flow Metab* 20: 1632–1635, 2000.
18. Dunn JF and Swartz HM. In vivo electron paramagnetic resonance oximetry with particulate materials. *Methods* 30: 159–166, 2003.
19. Duong TQ, Iadecola C, and Kim SG. Effect of hyperoxia, hypercapnia, and hypoxia on cerebral interstitial oxygen tension and cerebral blood flow. *Magn Reson Med* 45: 61–70, 2001.
20. Eidelberg D, Johnson G, Tofts PS, Dobbin J, Crockard HA, and Plummer D. ^{19}F imaging of cerebral blood oxygenation in experimental middle cerebral artery occlusion: preliminary results. *J Cereb Blood Flow Metab* 8: 276–281, 1988.
21. Feng ZC, Roberts EL Jr, Sick TJ, and Rosenthal M. Depth profile of local oxygen tension and blood flow in rat cerebral cortex, white matter and hippocampus. *Brain Res* 445: 280–288, 1988.
22. Ferrari M, Wilson DA, Hanley DF, Hartmann JF, Rogers MC, and Traystman RJ. Noninvasive determination of hemoglobin saturation in dogs by derivative near-infrared spectroscopy. *Am J Physiol* 256: H1493–H1499, 1989.
23. Fiat D, Ligeti L, Lyon RC, Ruttner Z, Pekar J, Moonen CTW, and McLaughlin AC. In vivo ^{17}O NMR study of rat brain during ^{17}O inhalation. *Magn Reson Med* 24: 370–374, 1992.
24. Frostig RD, Lieke EE, Ts'o DY, and Grinvald A. Cortical functional architecture and local coupling between neuronal activity and the microcirculation revealed by *in vivo* high-resolution optical imaging of intrinsic signals. *Proc Natl Acad Sci USA* 87: 6082–6086, 1990.
25. Gleichmann U, Ingvar DH, Lübbers DW, Siesjo BK, and Thews G. Tissue pO_2 and pCO_2 of the cerebral cortex, related to blood gas tensions. *Acta Physiol Scand* 55: 127–138, 1962.
26. Grieb P, Forster RE, Strome D, Goodwin CW, and Pape PC. O_2 exchange between blood and brain tissues studied with $^{18}O_2$ indicator-dilution technique. *J Appl Physiol* 58: 1929–1941, 1985.
27. Grinberg OY, Smirnov AI, and Swartz HM. High spatial resolution multi-site EPR oximetry: the use of convolution-based fitting method. *J Magn Reson* 152: 247–258, 2001.
28. Hou H, Grinberg OY, Taie S, Leichtweis S, Miyake M, Grinberg S, Xie H, Csete M, and Swartz HM. Electron paramagnetic resonance assessment of brain tissue oxygen tension in anesthetized rats. *Anesth Analg* 96: 1467–72, 2003.
29. Ingvar DH, Lübbers DW, and Siesjö B. Measurement of oxygen tension on the surface of the cerebral cortex of the cat during hyperoxia and hypoxia. *Acta Physiol Scand* 48: 373–381, 1960.
30. Jöbsis FF. Noninvasive, infrared monitoring of cerebral and myocardial oxygen sufficiency and circulatory parameters. *Science* 198: 1264–1267, 1977.
31. Jöbsis FF, Keizer JH, LaManna JC, and Rosenthal M. Reflectance spectrophotometry of cytochrome aa_3 in vivo. *J Appl Physiol* 43: 858–872, 1977.
32. Jones CE, Crowell JW, and Smith EE. Special communications: determination of mean tissue oxygen tensions by implanted perforated capsules. *J Appl Physiol* 26: 630–633, 1969.
33. Kautsky H. Quenching of luminescence by oxygen. *Trans Faraday Soc* 35: 216–219, 1939.
34. Kim SG and Ugurbil K. Comparison of blood oxygenation and cerebral blood flow effects in fMRI: estimation of relative oxygen consumption change. *Magn Reson Med* 38: 59–65, 1997.
35. Kim SG and Ugurbil K. Functional magnetic resonance imaging of the human brain. *J Neurosci Methods* 74: 229–243, 1997.
36. Knopp JA and Longmuir IS. Intracellular measurement of oxygen by quenching of fluorescence of pyrenebutyric acid. *Biochim Biophys Acta* 279: 393–397, 1972.
37. Kreisman NR, Sick TJ, and Bruley DF. Local oxygen tension and its relationship to unit activity during penicillin interictal discharges in the bullfrog hippocampus. *Electroencephalogr Clin Neurophysiol* 46: 619–633, 1979.
38. Kreisman NR, Sick TJ, LaManna JC, and Rosenthal M. Local tissue oxygen tension-cytochrome a,a_3 redox relationships in rat cerebral cortex in vivo. *Brain Res* 218: 161–174, 1981.
39. Krogh A. The rate of diffusion of gases through animal tissues with some remarks on the coefficient of invasion. *J Physiol (*Lond) 52: 391–408, 1919.
40. Kuppusamy P, Shankar RA, and Zweier JL. In vivo measurement of arterial and venous oxygenation in the rat using 3D spectral-spatial electron paramagnetic resonance imaging. *Phys Med Biol* 43: 1837–1844, 1998.
41. Kwong KK, Belliveau JW, Chesler DA, Goldberg IE, Weisskoff RM, Poncelet BP, Kennedy DN, Hoppel BE, Cohen MS, and Turner R. Dynamic magnetic resonance imaging of human brain activity during primary sensory stimulation. *Proc Natl Acad Sci U S A* 89: 5675–5679, 1992.
42. LaManna JC and McCracken KA. Carbonic anhydrase inhibition and cerebral cortical oxygenation in the rat. *Adv Exp Med Biol* 277: 335–343, 1990.
43. LaManna JC, McCracken KA, Patil M, and Prohaska O. Brain tissue temperature: activation-induced changes determined with a new multisensor probe. *Adv Exp Med Biol* 222: 383–389, 1988.
44. LaManna JC, McCracken KA, Patil M, and Prohaska OJ. Stimulus activated changes in brain tissue temperature in the anesthetized rat. *Metab Brain Dis* 4: 225–237, 1989.
45. LaManna JC, Sick TJ, Pikarsky SM, and Rosenthal M. Detection of an oxidizable fraction of cytochrome oxidase in intact rat brain. *Am J Physiol* 253: C477–C483, 1987.
46. Lei H, Grinberg O, Nwaigwe CI, Hou HG, Williams H, Swartz HM, and Dunn JF. The effects of ketamine-xylazine anesthesia on cerebral blood flow and oxygenation observed using nuclear magnetic resonance perfusion imaging and electron paramagnetic resonance oximetry. *Brain Res* 913: 174–179, 2001.
47. Leniger-Follert E and Lübbers DW. Behavior of microflow and local pO_2 of the brain cortex during and after direct electrical stimulation. *Pflugers Arch* 366: 39–44, 1976.
48. Leniger-Follert E, Lübbers DW, and Wrabetz W. Regulation of local tissue P_{O2} of the brain cortex at different arterial O_2 pressures. *Pflugers Arch* 359: 81–95, 1975.
49. Lindauer U, Gethmann J, Kuhl M, Kohl-Bareis M, and Dirnagl U. Neuronal activity-induced changes of local cerebral microvascular blood oxygenation in the rat: effect of systemic hyperoxia or hypoxia. *Brain Res* 975: 135–140, 2003.
50. Liu KJ, Bacic G, Hoopes PJ, Jiang J, Du H, Ou LC, Dunn JF, and Swartz HM. Assessment of cerebral pO_2 by EPR oximetry in rodents: effects of anesthesia, ischemia, and breathing gas. *Brain Res* 685: 91–98, 1995.
51. Liu KJ, Gast P, Moussavi M, Norby SW, Vahidi N, Walczak T, Wu M, and Swartz HM. Lithium phthalocyanine: a probe for electron paramagnetic resonance oximetry in viable biological systems. *Proc Natl Acad Sci U S A* 90: 5438–5442, 1993.
52. Liu S, Liu W, Ding W, Miyake M, Rosenberg GA, and Liu KJ. Electron paramagnetic resonance-guided normobaric hyperoxia treatment protects the brain by maintaining penumbral oxygenation in a rat model of transient focal cerebral ischemia. *J Cereb Blood Flow Metab* 26: 1274–1284, 2006.
53. Liu S, Shi H, Liu W, Furuichi T, Timmins GS, and Liu KJ. Interstitial pO_2 in ischemic penumbra and core are differentially affected following transient focal cerebral ischemia in rats. *J Cereb Blood Flow Metab* 24: 343–349, 2004.
54. Liu S, Timmins GS, Shi H, Gasparovic CM, and Liu KJ. Application of in vivo EPR in brain research: monitoring tissue oxygenation, blood flow, and oxidative stress. *NMR Biomed* 17: 327–334, 2004.
55. Lothman E, LaManna JC, Cordingley G, Rosenthal M, and Somjen G. Responses of electrical potential, potassium levels, and oxidative metabolic activity of the cerebral neocortex of cats. *Brain Res* 88: 15–36, 1975.
56. Lothman EW and Somjen GG. Extracellular potassium activity, intracellular and extracellular potential responses in the spinal cord. *J Physiol (Lond)* 252: 115–136, 1975.
57. Lübbers DW. The meaning of the tissue oxygen distribution curve

and its measurement by means of Pt electrodes. *Prog Resp Res* 3: 112–123, 1969.
58. Lübbers DW. Oxygen delivery and microcirculation in the brain. In: *Microcirculation in Circulatory Disorders*, edited by Manabe H, Zweifach BW, and Messmer K. Tokyo: Springer-Verlag, 1988, pp. 33–50.
59. Lübbers DW and Baumgärtl H. Heterogeneities and profiles of oxygen pressure in brain and kidney as examples of the pO_2 distribution in the living tissue. *Kidney Int* 51: 372–380, 1997.
60. Lübbers DW and Opitz N. [The pCO_2-/pO_2-optode: a new probe for measurement of pCO_2 or pO_2 in fluids and gases (authors transl)]. *Z Naturforsch [C]* 30: 532–533, 1975.
61. Lux HD and Neher E. The equilibrium time course of $[K^+]_o$ in cat cortex. *Exp Brain Res* 17: 190–205, 1973.
62. Madsen PL and Secher NH. Near-infrared oximetry of the brain. *Prog Neurobiol* 58: 541–560, 1999.
63. Metzger H. Effects of direct stimulation on cerebral cortex oxygen tension level. *Microvasc Res* 17: 80–89, 1979.
64. Metzger H, Erdmann W, and Thews G. Effect of short periods of hypoxia, hyperoxia, and hypercapnia on brain O_2 supply. *J Appl Physiol* 31: 751–759, 1971.
65. Mitnick MH and Jöbsis FF. Pyrenebutyric acid as an optical oxygen probe in the intact cerebral cortex. *J Appl Physiol* 41: 593–597, 1976.
66. Nair P, Whalen WJ, and Buerk D. PO_2 of cat cerebral cortex: response to breathing N_2 and 100 per cent O_2. *Microvasc Res* 9: 158–165, 1975.
67. Nwaigwe CI, Roche MA, Grinberg O, and Dunn JF. Brain tissue and sagittal sinus pO_2 measurements using the lifetimes of oxygen-quenched luminescence of a ruthenium compound. *Adv Exp Med Biol* 530: 101–111, 2003.
68. Obrig H and Villringer A. Beyond the visible: imaging the human brain with light. *J Cereb Blood Flow Metab* 23: 1–18, 2003.
69. Offenhauser N, Thomsen K, Caesar K, and Lauritzen M. Activity-induced tissue oxygenation changes in rat cerebellar cortex: interplay of postsynaptic activation and blood flow. *J Physiol (Lond)* 565: 279–294, 2005.
70. Ogawa S, Lee TM, Kay AR, and Tank DW. Brain magnetic resonance imaging with contrast dependent on blood oxygenation. *Proc Natl Acad Sci U S A* 87: 9868–9872, 1990.
71. Ogawa S, Tank DW, Menon R, Ellermann JM, Kim SG, Merkle H, and Ugurbil K. Intrinsic signal changes accompanying sensory stimulation: functional brain mapping with magnetic resonance imaging. *Proc Natl Acad Sci U S A* 89: 5951–5955, 1992.
72. Opitz N and Lübbers DW. Theory and development of fluorescence-based optochemical oxygen sensors: oxygen optodes. *Int Anesthesiol Clin* 25: 177–197, 1987.
73. Owens G, Belmusto L, and Woldring S. Experimental intracerebral pO_2 and pCO_2 monitoring by mass spectrography. *J Neurosurg* 30: 110–115, 1969.
74. Pekar J, Ligeti L, Ruttner Z, Lyon RC, Sinnwell TM, van Gelderen P, Fiat D, Moonen CTW, and McLaughlin AC. In vivo measurement of cerebral oxygen consumption and blood flow using ^{17}O magnetic resonance imaging. *Magn Reson Med* 21: 313–319, 1991.
75. Prohaska OJ, Kohl F, Goiser P, Olcaytug F, Urban G, Jachimowicz A, Pirker K, Chu W, Patil M, LaManna J, and Vollmer R. Multiple chamber-type probe for biomedical application. In: International Conference on Solid-State Sensors and Actuators: Digest of Technical Papers. Piscataway, NJ: *IEEE*, 812–815, 1987.
76. Prohaska OJ, Olcaytug F, Pfunder P, and Dragaun H. Thin-film multiple electrode probes: possibilities and limitations. *IEEE Trans Biomed Eng* 33: 223–229, 1986.
77. Raichle ME. Behind the scenes of functional brain imaging: a historical and physiological perspective. *Proc Natl Acad Sci USA* 95: 765–772, 1998.
78. Raichle ME and Mintun MA. Brain work and brain imaging. *Annu Rev Neurosci* 29: 449–476, 2006.
79. Roberts M and Owens G. Direct mass spectrographic measurement of regional intracerebral oxygen, carbon dioxide, and argon. *J Neurosurg* 37: 706–710, 1972.
80. Rolett EL, Azzawi A, Liu KJ, Yongbi MN, Swartz HM, and Dunn JF. Critical oxygen tension in rat brain: a combined (31)P-NMR and EPR oximetry study. *Am J Physiol Regul Integr Comp Physiol* 279: R9–R16, 2000.
81. Rosenthal M and Jöbsis FF. Intracellular redox changes in functioning cerebral cortex, II: effects of direct cortical stimulation. *J Neurophysiol* 34: 750–762, 1971.
82. Rosenthal M, LaManna JC, Jöbsis FF, Levasseur JE, Kontos HA, and Patterson JL Jr. Effects of respiratory gases on cytochrome a in intact cerebral cortex: is there a critical PO_2? *Brain Res* 108: 143–154, 1976.
83. Rumsey WL, Vanderkooi JM, and Wilson DF. Imaging of phosphorescence: a novel method for measuring oxygen distribution in perfused tissue. *Science* 241: 1649–1651, 1988.
84. Severinghaus JW, Weiskopf RB, Nishimura M, and Bradley AF. Oxygen electrode errors due to polarographic reduction of halothane. *J Appl Physiol* 31: 640–642, 1971.
85. Seyde WC and Longnecker DE. Cerebral oxygen tension in rats during deliberate hypotension with sodium nitroprusside, 2-chloroadenosine, or deep isoflurane anesthesia. *Anesthesiology* 64: 480–485, 1986.
86. Seylaz J and Pinard E. Continuous measurement of gas partial pressures in intracerebral tissue. *J Appl Physiol* 44: 528–533, 1978.
87. Seylaz J, Pinard E, Meric P, and Correze J-L. Local cerebral P_{O2}, P_{CO2}, and blood flow measurements by mass spectrometry. *Am J Physiol* 245: H513–H518, 1983.
88. Sick TJ and Kreisman NR. Local tissue oxygen tension as an index of changes in oxidative metabolism in the bullfrog optic tectum. *Brain Res* 169: 575–579, 1979.
89. Sick TJ, Lutz PL, LaManna JC, and Rosenthal M. Comparative brain oxygenation and mitochondrial redox activity in turtles and rats. *J Appl Physiol* 53: 1354–1359, 1982.
90. Silver IA. Some observations on the cerebral cortex with an ultramicro, membrane-covered, oxygen electrode. *Med Electron Biol Eng* 3: 377–387, 1965.
91. Smith RH, Guilbeau EJ, and Reneau DD. The oxygen tension field within a discrete volume of cerebral cortex. *Microvasc Res* 13: 233–240, 1977.
92. Sugioka K and Davis DA. Hyperventilation with oxygen: a possible cause of cerebral hypoxia. *Anesthesiology* 21: 135–143, 1960.
93. Tammela OK, Lajevardi N, Huang CC, Wilson DF, Ivoria-Papadopoulos M, and Pastuszko A. The effects of induced apneic episodes on cerebral cortical oxygenation in newborn piglets. *Brain Res* 741: 160–165, 1996.
94. Ter-Pogossian M, Spratt JS Jr, Rudman S, and Spencer A. Radioactive oxygen 15 in study of kinetics of oxygen of respiration. *Am J Physiol* 201: 582–586, 1961.
95. Ter-Pogossian MM and Herscovitch P. Radioactive oxygen-15 in the study of cerebral blood flow, blood volume, and oxygen metabolism. *Semin Nucl Med* 15: 377–394, 1985.
96. Thews G. [A method for determination of oxygen diffusion coefficients, oxygen conductivity and oxygen solubility coefficients in brain tissue.]. *Pflugers Arch Gesamte Physiol Menschen Tiere* 271: 227–244, 1960.
97. Vanderkooi JM, Erecinska M, and Silver IA. Oxygen in mammalian tissue: methods of measurement and affinities of various reactions. *Am J Physiol* 260: C1131–C1150, 1991.
98. Vanzetta I and Grinvald A. Increased cortical oxidative metabolism due to sensory stimulation: implications for functional brain imaging. *Science* 286: 1555–1558, 1999.
99. Vaughan WM and Weber G. Oxygen quenching of pyrenebutyric acid fluorescence in water: a dynamic probe of the microenvironment. *Biochemistry* 9: 464–473, 1970.
100. Villringer A and Dirnagl U. Coupling of brain activity and cerebral blood flow: basis of functional neuroimaging. *Cerebrovasc Brain Metab Rev* 7: 240–276, 1995.
101. Villringer A, Planck J, Hock C, Schleinkofer L, and Dirnagl U. Near infrared spectroscopy (NIRS): a new tool to study hemody-

namic changes during activation of brain function in human adults. *Neurosci Lett* 154: 101–104, 1993.
102. Whalen WJ, Ganfield R, and Nair P. Effects of breathing O_2 or $O_2 + CO_2$ and of the injection of neurohumors on the PO_2 of cat cerebral cortex. *Stroke* 1: 194–200, 1970.
103. Wilson DF, Pastuszko A, DiGiacomo JE, Pawlowski M, Schneiderman R, and Delivoria-Papadopoulos M. Effect of hyperventilation on oxygenation of the brain cortex of newborn piglets. *J Appl Physiol* 70: 2691–2696, 1991.
104. Yokoyama H, Itoh O, Aoyama M, Obara H, Ohya H, and Kamada H. In vivo EPR imaging by using an acyl-protected hydroxylamine to analyze intracerebral oxidative stress in rats after epileptic seizures. *Magn Reson Imaging* 18: 875–879, 2000.
105. Zhu XH, Zhang N, Zhang Y, Zhang X, Ugurbil K, and Chen W. In vivo ^{17}O NMR approaches for brain study at high field. *NMR Biomed* 18: 83–103, 2005.

Address reprint requests to:
Joseph C. LaManna, PhD
Department of Anatomy
Case Western Reserve University
School of Medicine
10900 Euclid Avenue
Cleveland, OH 44106-4930

E-mail: joseph.lamanna@case.edu

Date of first submission to ARS Central, February 28, 2007; date of final revised submission, February 28, 2007; date of acceptance, March 8, 2007.

This article has been cited by:

1. Sandra W. Chan, Rachael A. Dunlop, Anthony Rowe, Kay L. Double, Kenneth J. Rodgers. 2012. l-DOPA is incorporated into brain proteins of patients treated for Parkinson's disease, inducing toxicity in human neuroblastoma cells in vitro. *Experimental Neurology* **238**:1, 29-37. [CrossRef]
2. Longxuan Li, Jennifer Welser-Alves, Arjan van der Flier, Amin Boroujerdi, Richard O. Hynes, Richard Milner. 2012. An angiogenic role for the #5#1 integrin in promoting endothelial cell proliferation during cerebral hypoxia. *Experimental Neurology* **237**:1, 46-54. [CrossRef]
3. Andrew A. V. Hill, John Simmers, Pierre Meyrand, Jean-Charles Massabuau. 2012. Modulation of network pacemaker neurons by oxygen at the anaerobic threshold. *Journal of Comparative Physiology A* **198**:7, 511-523. [CrossRef]
4. Mayumi Kajimura, Tsuyoshi Nakanishi, Toshiki Takenouchi, Takayuki Morikawa, Takako Hishiki, Yoshinori Yukutake, Makoto Suematsu. 2012. Gas biology: Tiny molecules controlling metabolic systems. *Respiratory Physiology & Neurobiology* . [CrossRef]
5. T. Morikawa, M. Kajimura, T. Nakamura, T. Hishiki, T. Nakanishi, Y. Yukutake, Y. Nagahata, M. Ishikawa, K. Hattori, T. Takenouchi, T. Takahashi, I. Ishii, K. Matsubara, Y. Kabe, S. Uchiyama, E. Nagata, M. M. Gadalla, S. H. Snyder, M. Suematsu. 2012. Hypoxic regulation of the cerebral microcirculation is mediated by a carbon monoxide-sensitive hydrogen sulfide pathway. *Proceedings of the National Academy of Sciences* . [CrossRef]
6. Sune N Jespersen, Leif Østergaard. 2011. The roles of cerebral blood flow, capillary transit time heterogeneity, and oxygen tension in brain oxygenation and metabolism. *Journal of Cerebral Blood Flow & Metabolism* . [CrossRef]
7. Klaus Ulrich Klein, Stefan Boehme, Erik Kristopher Hartmann, Marc Szczyrba, Matthias David, Klaus Markstaller, Kristin Engelhard. 2011. A Novel Technique for Monitoring of Fast Variations in Brain Oxygen Tension Using an Uncoated Fluorescence Quenching Probe (Foxy AL-300). *Journal of Neurosurgical Anesthesiology* **23**:4, 341-346. [CrossRef]
8. K. U. Klein, K. Fukui, P. Schramm, A. Stadie, G. Fischer, C. Werner, J. Oertel, K. Engelhard. 2011. Human cerebral microcirculation and oxygen saturation during propofol-induced reduction of bispectral index. *British Journal of Anaesthesia* . [CrossRef]
9. Ville R.I. Kaila, Esko Oksanen, Adrian Goldman, Dmitry A. Bloch, Michael I. Verkhovsky, Dage Sundholm, Mårten Wikström. 2011. A combined quantum chemical and crystallographic study on the oxidized binuclear center of cytochrome c oxidase. *Biochimica et Biophysica Acta (BBA) - Bioenergetics* **1807**:7, 769-778. [CrossRef]
10. Jérôme Lecoq, Alexandre Parpaleix, Emmanuel Roussakis, Mathieu Ducros, Yannick Goulam Houssen, Sergei A Vinogradov, Serge Charpak. 2011. Simultaneous two-photon imaging of oxygen and blood flow in deep cerebral vessels. *Nature Medicine* **17**:7, 893-898. [CrossRef]
11. Aude Carreau, Bouchra El Hafny-Rahbi, Agata Matejuk, Catherine Grillon, Claudine Kieda. 2011. Why is the partial oxygen pressure of human tissues a crucial parameter? Small molecules and hypoxia. *Journal of Cellular and Molecular Medicine* **15**:6, 1239-1253. [CrossRef]
12. Silke Musa, Danielle R. Rand, Carmen Bartic, Wolfgang Eberle, Bart Nuttin, Gustaaf Borghs. 2011. Coulometric Detection of Irreversible Electrochemical Reactions Occurring at Pt Microelectrodes Used for Neural Stimulation. *Analytical Chemistry* **83**:11, 4012-4022. [CrossRef]
13. Dale A. Pelligrino, Francesco Vetri, Hao-Liang Xu. 2011. Purinergic mechanisms in gliovascular coupling. *Seminars in Cell & Developmental Biology* **22**:2, 229-236. [CrossRef]
14. Francesca Faggioli, Jan Vijg, Cristina Montagna. 2011. Chromosomal aneuploidy in the aging brain. *Mechanisms of Ageing and Development* . [CrossRef]
15. R. E. Haskew-Layton, T. C. Ma, R. R. Ratan. 2011. Reply to Bell et al.: Nrf2-dependent and -independent mechanisms of astrocytic neuroprotection. *Proceedings of the National Academy of Sciences* **108**:1, E3-E4. [CrossRef]
16. Jesús Pacheco-Torres, Pilar López-Larrubia, Paloma Ballesteros, Sebastián Cerdán. 2011. Imaging tumor hypoxia by magnetic resonance methods. *NMR in Biomedicine* **24**:1, 1-16. [CrossRef]
17. Jakob H. Lagerlo#f, Jon Kindblom, Peter Bernhardt. 2011. 3D modeling of effects of increased oxygenation and activity concentration in tumors treated with radionuclides and antiangiogenic drugs. *Medical Physics* **38**:8, 4888. [CrossRef]
18. Obinna I. Ndubuizu, Constantinos P. Tsipis, Ang Li, Joseph C. LaManna. 2010. Hypoxia-inducible factor-1 (HIF-1)-independent microvascular angiogenesis in the aged rat brain. *Brain Research* **1366**, 101-109. [CrossRef]

19. Stuart F Cogan, Julia Ehrlich, Timothy D Plante, Marcus D Gingerich, Douglas B Shire. 2010. Contribution of Oxygen Reduction to Charge Injection on Platinum and Sputtered Iridium Oxide Neural Stimulation Electrodes. *IEEE Transactions on Biomedical Engineering* **57**:9, 2313-2321. [CrossRef]
20. Dominik W Schelshorn, Armin Schneider, Wolfgang Kuschinsky, Daniela Weber, Carola Krüger, Tanjew Dittgen, Heinrich F Bürgers, Fatemeh Sabouri, Nikolaus Gassler, Alfred Bach, Martin H Maurer. 2009. Expression of hemoglobin in rodent neurons. *Journal of Cerebral Blood Flow & Metabolism* **29**:3, 585-595. [CrossRef]
21. Jeoung Hyuk Lee, Younsuk Lee, Junyong In, Seung-Hyun Chung, Hong-il Shin, Kyoungjin Lee, Kyoung Ok Kim, Hun Cho. 2009. Response of cerebral oximetry to increase in alveolar concentration of desflurane: effect of remifentanil and cerebrovascular CO2 reactivity. *Korean Journal of Anesthesiology* **56**:5, 543. [CrossRef]
22. Kazuto Masamoto, Kazuo Tanishita. 2009. Oxygen Transport in Brain Tissue. *Journal of Biomechanical Engineering* **131**:7, 074002. [CrossRef]
23. Gerald A. Dienel, Nancy F. Cruz. 2008. Imaging Brain Activation. *Annals of the New York Academy of Sciences* **1147**:1, 139-170. [CrossRef]
24. Yilong Ma, Shufen Wu. 2008. Simultaneous measurement of brain tissue oxygen partial pressure, temperature, and global oxygen consumption during hibernation, arousal, and euthermy in non-sedated and non-anesthetized Arctic ground squirrels. *Journal of Neuroscience Methods* **174**:2, 237-244. [CrossRef]
25. Mark O. Bevensee, Walter F. Boron. 2008. Effects of acute hypoxia on intracellular-pH regulation in astrocytes cultured from rat hippocampus. *Brain Research* **1193**, 143-152. [CrossRef]
26. Harold M. Swartz . 2007. On Tissue Oxygen and Hypoxia. *Antioxidants & Redox Signaling* **9**:8, 1111-1114. [Citation] [Full Text PDF] [Full Text PDF with Links]